American Journal of Nanomaterials, 2017, Vol. 5, No. 1, 31-42
Available online at http://pubs.sciepub.com/ajn/5/1/5

DOI:10.12691/ajn-5-1-5

Antibacterial Applications of Anatase TiO_2 Nanoparticle

Hani A. Alhadrami[1,2,3,#], Aisha Baqasi[1,#], Javed Iqbal[4,#], Raniyah A.M. Shoudri[1], Ahmad Mohammad Ashshi[5], Esam I. Azhar[1,2], Faten Al-Hazmi[6], Ahmed Al-Ghamdi[6], S. Wageh[6,7,#,*]

[1]Faculty of Applied Medical Sciences, Department of Medical Laboratory Technology, King Abdulaziz University, P. O. Box 80402 Jeddah 21589, Saudi Arabia
[2]Special Infectious Agents Unit, King Fahd Medical Research Centre, King Abdulaziz University, P. O. Box 80402 Jeddah 21589, Saudi Arabia
[3]Center of Innovation in Personalized Medicine, King Fahd Medical Research Center, King Abdulaziz University, P. O. Box 80402, Jeddah, 21589, Kingdom of Saudi Arabia
[4]Center of Nanotechnology, King Abdulaziz University, Jeddah 21589, Saudia Arabia
[5]Department of Laboratory Medicine, Faculty of Applied Medical Sciences, Umm Al-Qura University, P.O. Box 7607, Makkah, Saudi Arabia
[6]Department of Physics, Faculty of Science, King Abdulaziz University, Jeddah, 21589, Saudi Arabia
[7]Physics and Engineering Mathematics Department, Faculty of Electronic Engineering, Menoufia University, Menouf, 32952, Egypt
[#]These authors have equally contributed in writing the manuscript.
*Corresponding author: iqbaljavedch@gmail.com

Abstract Many methods have been used for the preparation of nanostructured metal oxides. Here we report the synthesis of TiO_2 nanoparticles by facile hydrothermal process by varying the concentration of the precursor and reaction temperature while keeping the process time constant. Morphological, structural and optical studies were carried out by scanning electron microscopy equipped with energy dispersive spectroscopy, X-ray powder diffraction spectroscopy and VU-Vis-NIR spectroscopy. Morphological and compositional analysis reveal that the prepared nanoparticles are highly pure with an approximate average particle size 5-15nm. XRD studies showed their crystalline structure and the sizes around 5 nm, while the optical absorption studies in the photon wavelength range 300-600 nm reveal that the strong absorbance peak is positioned at around 3.5 eV nm whereas visible energy is almost transparent for the materials. Finally, the antibacterial effect of TiO_2 nanoparticles has been studied. Plating technique was used to determine lowest concentration that prevent or inhibit growth of bacteria. This technique of TiO_2 nanoparticle was used against most common organisms which cause wound infection including: MRSA, *E. coli* and *Pseudomonas aeruginosa*. Different concentrations of TiO_2 nanoparticles were used 100 µg/ml, 200 µg/ml, 400 µg/ml, 600 µg/ml and 800 µg/ml. Inhibition of bacteria was different for prepared TiO_2 samples due to different concentration of the precursors and synthesis temperature.

Keywords: *TiO_2, nanoparticles, crystal structure, antibacterial*

Cite This Article: Hani A. Alhadrami, Aisha Baqasi, Javed Iqbal, Raniyah A.M. Shoudri, Ahmad Mohammad Ashshi, Esam I. Azhar, Faten Al-Hazmi, Ahmed Al-Ghamdi, and S. Wageh, "Antibacterial Applications of Anatase TiO_2 Nanoparticle." *American Journal of Nanomaterials*, vol. 5, no. 1 (2017): 31-42. doi: 10.12691/ajn-5-1-5.

1. Introduction

In the recent past, nanomaterials of different metal oxides have attracted much attention due to their variety of technological application they offer such as, catalysis, sensors, optoelectronics applications, solar cells, electroluminescent devices, light-emitting devices and environmental remediation [1-7]. Researchers have always been interested to synthesize different nanomaterials and exploit them in diverse applications to improve the quality and efficiency of the devices. As a matter of fact, nanoparticles (NPs) possess altogether distinctive properties compared to their bulk materials. Apart from their application in optoelectronics and environmental, nanoparticles have also been equally improving the quality of human life by exploiting them in life sciences. Metal oxide nanoparticles are of great interest for scientists to use them in medicine, pharmaceutical and biological applications [8,9]. Due to their low dimensions and high surface to volume ratio, NPs attach firmly with microbial membranes which play pivotal role for antibacterial efficiency [10]. In biomedical devices, the NPs are coated in the form of oxides to prevent bacterial proliferation and colonization due to their catalytic activity. They have successfully been exploited for the detection of proteins, production of drugs, purification and separation of cells and biological molecules and for the cure of tumors [11].

TiO_2 NPs have emerged as new generation of novel materials and of prime interest due to its applications in vast area of nanoscience because it is non-toxic and cost effective. The physical properties of TiO2 NPs largely

influence their applications [12]. It is found in three forms, i.e., brookit, anatase and rutile. Out of three, anatase NPs are commonly used for different applications such as, dye sensitized solar cells, gas sensors, photo degradation of organic compound, organic synthesis, deactivation of microorganisms and cell culture [13]. The restrictive performance of NPs generally follows mainly two pathways that are colligated to each other and may occur at the same instant. First, interruption of membrane potential and integrity and secondly, production of oxygen free radicals, i.e., NPs are acting as nanocatalyst [14]. TiO_2 NPs have been successfully synthesized by several methods, for example, sol-gel, precipitation, electrochemical, solvothermal, sonochemical, solid state reactions and microwave irradiation technique [15-21]. These processes involve environmentally unfriendly reagents which may cause biological hazards or toxicity.

In this study, TiO_2 spherical nanocrystallites with anatase crystal structures are synthesized by facile hydrothermal process, chemically and physically characterized, and their antibacterial activity has been investigated. The nanoparticles are tested in a dose response strategy against three of the most common pathogenic bacteria: Methicillin Resistance *Staphylococcus aureus* (MRSA), *E. coli* and *Pseudomonas aeruginosa* that cause wound infection. The impact of this work will give new strategies in treatment of wound infection.

2. Experimental

2.1. Preparation of TiO_2 Nanoparticles

Hydrothermal method has been known as an effective strategy for preparation of oxide nanoparticles both of binary and ternary compounds. This method has some advantages such as, low coast, low temperature, and simplicity of the setup. On the other hand, hydrothermal method has an important disadvantage which is the long-time of heating in autoclave. One of the methods of preparation can overcome of this disadvantage which is heating by microwave radiation. Preparation of nanostructures by microwave heating has more than one of advantages such as, increase of crystallinity without any additional post heat treatments, heating the materials under reaction need short time, consequently produce nanostructures with time and cost saving.

TiO_2 nanostructures were prepared by microwave heating systems. Microwaves have lower energy relative to other forms of electromagnetic energy and lie in frequency range from 300MHz to 300GHz corresponding to energies from 1.24×10-3 meV to 1.24 meV. Heating materials with microwave radiation take place by volumetric absorption of the lower electromagnetic energy and transform into heat of the material under expose. By this way, the generated heat inside the material not like conventional heating where the heat is distributing through the material from outside to inside by conduction. Consequently, the method of heating the materials by microwave has some advantages like as reducing processing time due to fast heating rate and homogeneity in heating process which lead to enhancing quality of material and compound produce by this method.

TiO_2 nanoparticles were prepared by hydrothermal condition as follow. Started with the solution of 0.08 M of $Ti[OCH(CH_3)_2]_4$ in de ionized water. The final solutions were adjusted to 25 mL in 50 mL Teflon vessel by adding Di-water, followed by sealing the vessel. The reactions for different samples were conducted at different temperatures in microwave oven and time was kept constant as 90 min, then subsequently, cooled to the room temperature slowly. Finally, TiO_2 nanopowders were collected by centrifugation and washed by water five times. The final powders dried in desiccator. Different conditions were used for preparation of TiO_2 and listed in Table 1.

Table 1. TiO_2 nanoparticles of different sizes prepared by changing the concentration of of Ti[OCH(CH3)2]4 precursor and the reaction temperature at constant time

Sample	Concentration of $Ti[OCH(CH_3)_2]_4$ (mmole/mL)	Temperature °C
Ti1	3.38	100
Ti2	1.96	100
Ti3	3.38	200
Ti4	1.96	200

2.2. Growth and Morphological Characteristic of Bacterial Strains

The growth of *Staphylococcus aureus* subsp. aureus (ATCC® 43300MINIPACK™), *Pseudomonas aeruginosa* (ATCC® 27853™) and *Escherichia coli* (ATCC® 25922™) were obtained from American Type Culture Collection (ATCC) org. (Manassas, USA). The bacterial strains were characterized by observing the optical density (OD) and colony forming units (CFUs) of the bacterial cells over time. Aseptic methods are necessary for managing all the microbiological works, which was achieved under laminar flow hood. A stock cultures of the bacteria were stored at (-20°C) in Trypticase Soy Agar/Broth (TSB) supplemented with 50 % sterile glycerol which used as cryopreservative. The bacterial strains were sub-cultured onto Luria Bertani (LB) agar plate from a 200 µL frozen glycerol stock by using a sterile inoculation loop. The sub-culture was incubated overnight at 37o C for 18 hours minimum. The LB ager and broth were purchased from Micromaster Laboratories Pvt. Ltd. (Maharashtra, India). The LB agar used for growing strains was supplemented with 10 gm/L casein enzymes hydrolysate, 5 gm/L yeast extract, 5 gm/L NaCl and 15 gm/L agar. Similar ingredients are existing in LB broth without agar. A 40 g of LB agar powder was dissolved in 1000 ml distilled water while preparation of LB broth was required 1 g of powder dissolved in 50 ml distilled water. The media of LB agar and broth were sterilized at 121°C in autoclave, then the agar medium was poured into sterilized petri-dishes and kept at room temperature for solidification. From the first agar plate, a single colony was streaked out on a new LB agar plate for preparing a second sub-culture which was incubated at 37°C overnight. For bacterial inoculum, a single colony from second sub-culture plate was inoculated in 100 ml Erlenmeyer flask containing 50 ml LB broth. The inoculum was incubated in a rotary shaker (GFL 3031 Shaking Incubator from UNIQUE Medical Laboratory Equipment

Trading & Services, Sharjah, United Arab Emirates) at 37°C at speed 150 rpm for 18 hours. The optimum growth of the overnight culture was observed by using a spectrophotometer (GENWSYS™10S UV-VIS Spectrophotometer from Thermo Fisher Scientific Inc., Madison, USA) to measure the optical density at 600 nm (OD600).

2.3. Preparation of Bacterial Suspension

The bacterial growth was monitored by measuring the turbidity of the LB broth media at OD600. After the overnight incubation, the bacterial cells were transferred into 50 ml polypropylene conical VWR® high-performance centrifuge tubes with flat or plug caps (VWR International, LLC Radnor, PA, USA) and harvested by centrifugation (High-Speed Refrigerated Centrifuges CR 22 GIII from Hitachi Koki Co., Ltd., Japan) at 5,000 rpm for 7 minutes at room temperature (22°C). The supernatant was discarded and the harvested pellet was washed three times with 10 ml of 0.9 % NaCl normal saline, which was purchased from Pharmaceutical Solutions Industry (PSI) (Jeddah, Saudi Arabia). The pellet in each washing were centrifuged for 7 minutes at 5,000 rpm at room temperature (22°C. After the third washing, the microbial stock solutions were prepared by re-suspending the final pellets in 10 ml of 0.9 % NaCl normal saline. Absorbance of the suspension was measured at OD600 to count the viable cells before adding the TiO_2 nanostructures [22].

2.4. Colony Counting of Bacterial Cells

The bacterial cells were divided into six tubes; each contains 5 ml of bacterial suspension. TiO_2 nanocrystallites were weighed at dose response manner (100, 200, 400, 600 and 800) µg using an analytical laboratory balance (XPE504DR from Mettler-Toledo International Inc, USA). There were several methods for nanoparticles sterilization. Thus, after measuring the different TiO_2 nanocrystallites doses, they were sterilized using UV light for 45 minutes [23]. The Control suspension was used without TiO_2 nanocrystallites. TiO_2 nanocrystallites were dissolved in 5 ml bacterial suspension at dose response manner and mix gently by vortex (Bench Mixer Benchmark Vortex Mixer from Science Lab Supplies, St. Augustine, FL). The bacterial growth was examined by measuring the OD600 after adding the TiO_2 nanocrystallites. Fritz et al. described the drop-plating method for counting the CFUs of bacterial cells [24]. At zero time, serial dilutions (1:10) from (10-1–10-8) were accomplished by diluting the bacterial cells (100µL) in micro-centrifuge tubes (SPL Life Sciences,Pocheon-si, Gyeonggi-do, Korea) consisting of sterile 0.9% NaCl normal saline (900µL) [25]. For the plating method, three 10µL aliquots of the proper dilution were dotted onto LB agar using an automatic pipette and incubated overnight at 37°C. The samples were re-incubated in a rotary shaker at 37°C at speed 150 rpm for several time intervals.

2.5. Growth Curves of Bacterial Cells Exposed to TiO_2 Quantum Dots

Bacterial cells growth happens in five phases: lag phase, exponential phase, stationary phase, death phase and extended or long-term stationary phase [26]. The growth curve was measured both viable and dead bacteria. The lag phase is the most unwell described phase and has been supposed to be a process of absence of bacterial growth for a period that's required to achieve the new medium. Some aspects may affect the bacterial growth during lag phase that vary among bacterial species or the period of cells stayed at starved conditions [27]. On the other hand, the exponential phase and stationary phase were representing the rate of cell division and termination of cell division, respectively. Stochastic death and programmed cell death was resulted when bacterial cells exhausted the nutrients in the medium. At this phase, the nutrients were released into environment from dead cells which allowed the survivors bacteria to use these constituents for their survival and entering in long-term stationary phase [28]. The bacterial cells from long-term stationary phase are capable of maintaining their constant cell density and stay viable for years in a batch culture without supplements [29]. The cells inoculated from this phase were revealed an extended lag phase in growth compared to their growth from late stationary phase [28]. Hence, the TiO_2 quantum dots were added at different doses to measure their effect on the growth of bacterial cells. At 1-hour time intervals, serial dilution was performed as previously described at time zero for samples recovered from the shaker and the growth was checked by measuring the OD600. Drop-plate method was implemented for the recovered samples by spotting 10µL aliquots in triplicates on LB agar and incubated at 37°C overnight. Samples were re-incubated in a rotary shaker at 37°C at speed 150 rpm which the similar protocol of dilution, drop-plating and measuring the OD600 was done for 2 hours, 3 hours and 24 hours. The experimental procedures were achieved for negative-control (without TiO_2 nanocrystallites) and the treatment samples (containing TiO_2 nanocrystallites) [30].

2.6. Determination of Minimum Exposure Time of Efficient Antimicrobial Activity of TiO_2 nanocrystallites

The dose response curve experiment was completed after the 24 hours when bacterial cells reached to the decline phase. The antimicrobial activity of bacterial strains against a range of known concentration of TiO_2 nanocrystallites after a period of time intervals was evaluated by counting the CFUs/ml to detect to minimum inhibitory concentration (MIC). The MIC was taken at a specific concentration required to arrest bacterial growth at a specific time. The bacterial growth was determined by plotting dose response curve of CFUs/ml and OD versus time. A comparison was made from the dose response curves to investigate the ideal TiO_2 nanocrystallites concentration that showed the antimicrobial effect at a certain exposure time [30].

2.7. Characterization

The morphology of prepared powder samples was analyzed by field emission scanning electron microscopy Jeol, Japan (FESEM- JSM-7600F), chemical compositions were measured by energy dispersive spectroscopy using a

FESEM attached with an Oxford EDS system. Whereas, the X-ray diffrectometer was used to analyze the crystalline nature and phase studies of the undoped and Zn-doped samples. Rigaku, Ultima-IV was used to perform the XRD measurements which is equipped with Cu-Kα radiation (λ=1.54060 nm) operated at 40 kV and 40 mA at room temperature. The XRD spectra were measured in the 2θ angular region between 10° to 80° and step size was kept 0.05°. Optical absorption spectra were measured using a UV–Vis–NIR spectroscopy (Jasco V-770 attached with 60 mm integrating sphere) in the spectral range 200–800 nm. Finally, plating technique was used to analyse the antibacterial activity of the prepared TiO_2 nanoparticles samples.

3. Results

3.1. Surface Morphological Studies

Surface morphological studies of the prepared TiO_2 samples (Ti1-4) were performed by scanning electron microscopy. Figure 1 shows the typical high magnification images of the as prepared TiO_2 nano-powder samples deposited on carbon stripe. Around the examining area, it can be noticed that the nanoparticles are densely aggregated in the form of big clusters but the approximate average size of the nanoparticles is 5-15nm and are semi spherical in shapes. It can be easily noticed from the SEM micrographs that except samples Ti1 where the particles size is little smaller than rest of the samples (Ti3, and Ti4) which were prepared at low temperature and high concentration and size of Ti1 sample also smaller than the sample high temperature and low concentration. However, over all there is small variation in the particle sizes of all four samples which may be due to the conditions applied for their synthesis.

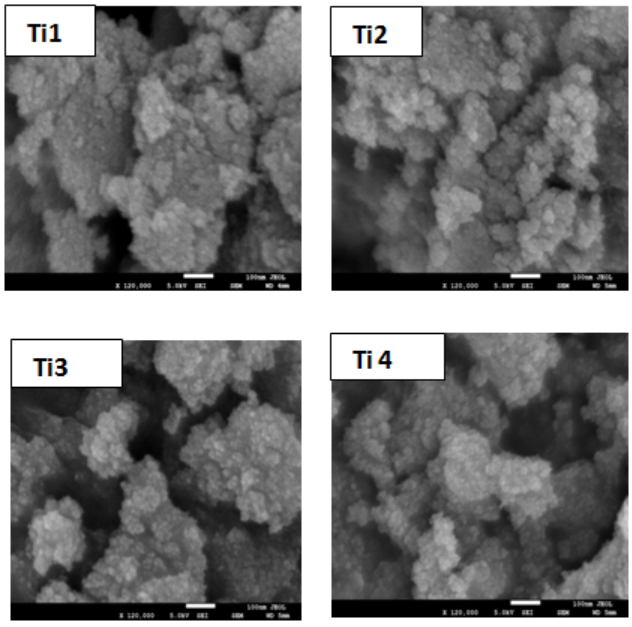

Figure 1. FESEM micrograph of TiO_2 nanoparticles samples. All the images were taken at magnification of 120k with SEI detector and the scale shown is 100 nm

3.2. Energy Dispersive X-ray Spectroscopy

Figure 2 shows the EDS spectrum of the as prepared TiO2 nanoparticles. All the spectra show that Ti and O are the only elements present in the samples which indicate that the prepared samples are highly pure. No impurity peaks present in all spectra of four samples. The elemental composition by weight percentage of the Ti and O varies in all samples and all samples showed non-stoichiometric compositions with increase of atomic and weight percentage of O relative to Ti. The ratios of weight percentages of O/Ti are presented in Table 2. Clearly, the samples that prepared at low temperature and that prepared with low concentrations have smaller O/Ti weight percentage ratios relative to the samples prepared at high temperatures with high concentration of Ti ions in the solution (Ti4).

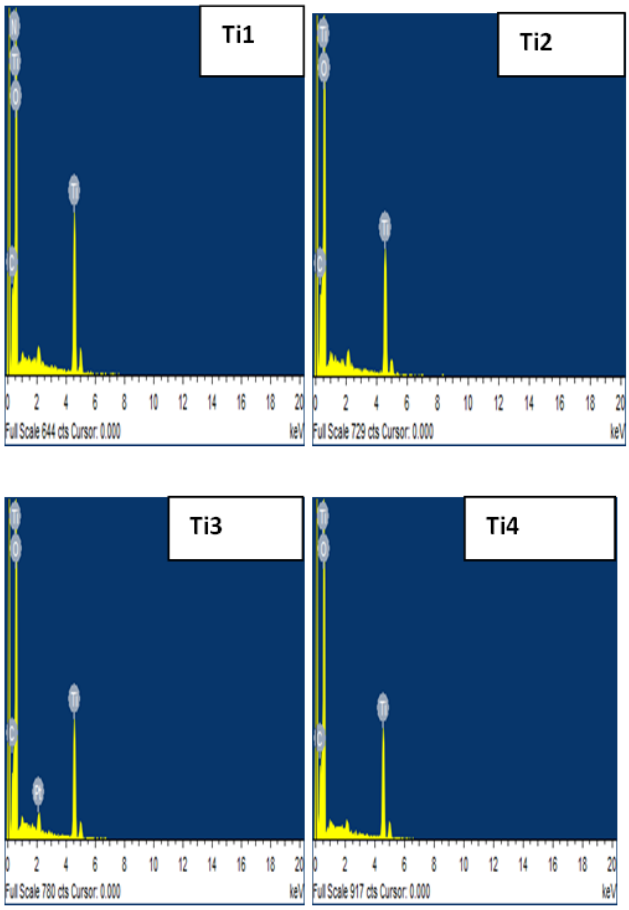

Figure 2. EDS micrograph of TiO_2 nanoparticles samples

3.3. Structural Analysis

The XRD patterns of different samples of TiO_2 obtained are shown in Figure 3. All the spectra clearly show the polycrystalline structure of the TiO_2 nanoparticles with different orientation along different planes. The diffraction lines in the XRD spectra are matching to the anatase crystalline phase of TiO_2 which are well indexed with the reference card No. ICCD-PDF 44309. It can be noticed in the spectra that only anatase phase is present in the sample. The broad peaks in the spectra indicate that the particle size is relatively small.

The peak intensities of the samples Ti3 is higher than those of Ti1, 2, 4, samples which may be due to slight changes in the grain size of the TiO_2. Crystallite size of the TiO_2 nanoparticles could be estimated using the following Scherrer equation:

$$D = \frac{K\lambda}{\beta \cos\theta}$$

where D is the crystallite size, K is the Scherrer constant equals to 0.9 for spherical shapes, λ is wavelength of the X-rays radiation, β is the full width at half maximum (FWHM) and θ is the Bragg's diffraction angel. The diffraction peaks appearing at 2θ of 25.3, 37.8, 47.8, 54.1, 62.6, 70.4 and 75.5 which correspond to phases (101), (103), (200), (105), (213), (116) and (107) respectively. From the XRD patterns, the calculated size of the nanocrystallites were found 4.99, 5.03, 6.47 and 5.36nm for samples Ti1, Ti2, Ti3 and Ti4 respectively, which has been exceeded the exciton Bohr diameter by about 1.5 nm. Obviously, the reported nanocrystallite sizes reveled that sample Ti1 has the smallest size which are compatible with the SEM results.

3.4. Optical Studies of the TiO_2 Nanoparticles

Optical absorbance is a powerful method to determine the energy gap and particle size as well as optical properties of the samples. The useful semiconductors for photocatalysis have a band gap comparable to the energy of the photons of visible or ultraviolet light, having a value of Eg < 3.5 eV. The majority of authors have determined that in TiO_2 the rutile has a direct band gap of 3.06 eV and an indirect one of 3.10 eV and the anatase has only an indirect band gap of 3.23 eV [31,32]. However, Reddy
from the plot for indirect transition are quite low (2.95 – 2.98 eV) [31].

Table 2. O/Ti weight percentage ratio, band gaps and calculated nanocrystallite sizes from XRD measurements

Sample	O/Ti weight percentage ratio	Scherer Size (Å)	Band gap (eV)
Ti1	1.05	49.9	3.5
Ti2	1.18	50.3	3.44
Ti3	1.19	64.7	3.42
Ti4	1.23	53.6	3.43

Contrary to the other authors, to conclude that the direct transition is more favorable for TiO_2 nanoparticles with anatase phase. There have been reported values in the literature from 2.86 to 3.34 eV for the anatase phase. Here in, UV–Vis absorption spectra were taken in the photon wavelength range between 300 and 600 nm. Figure 4 shows the UV-Vis absorption spectrum of hyderothermally synthesized TiO_2 nanoparticles. As in Figure 4 the optical absorption peak has been found at between 350 nm to 362 nm. The band gaps were obtained from the second derivative of the absorption spectra, and are listed in Table 2.

Clearly, the band gaps increasing with decreasing nanoparticles size and Ti1 sample with smallest nanocrystallite size has the largest band gap. The band gap of the nanocrystallites are blue shifted relative to bulk band gap of TiO_2. This result in agreement with the previous results that showed the existence of the blue shift for TiO_2 nanocrystallites [33].

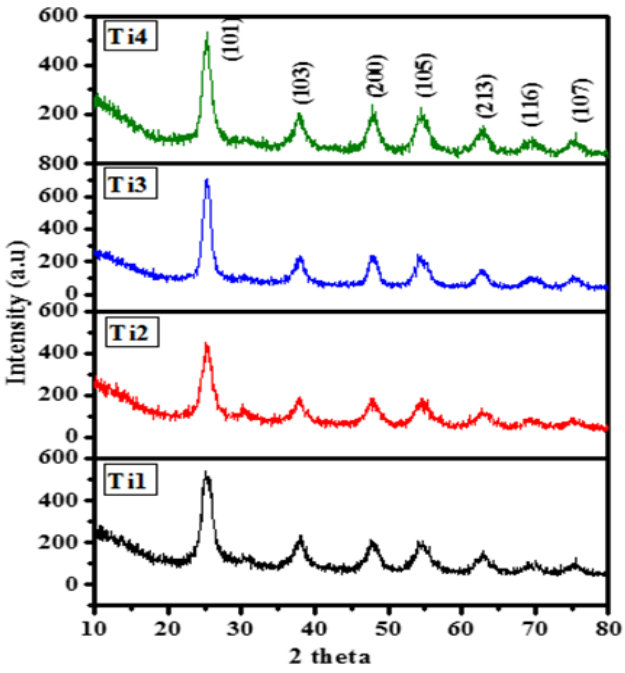

Figure 3. XRD spectra of different sizes of TiO_2 nanoparticles

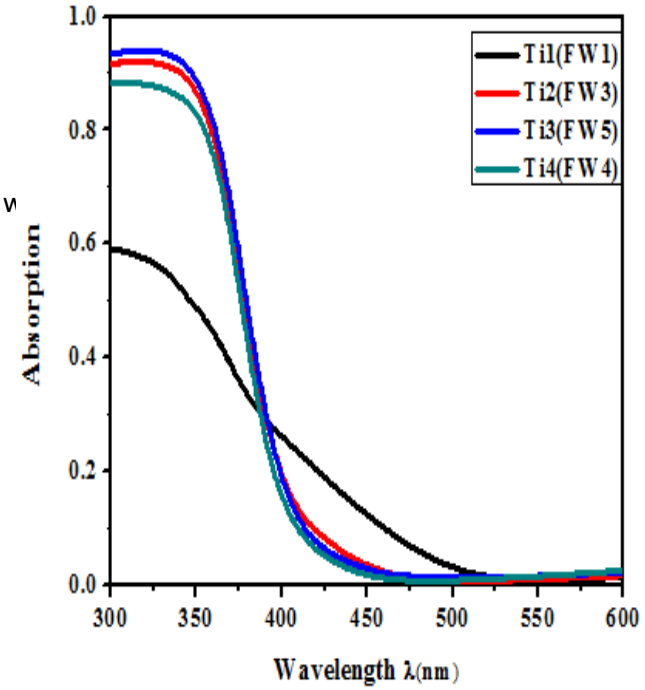

Figure 4. Optical absorption curves of TiO_2 nanoparticles prepared by hydrothermal process

3.5. Plating Technique for Bacteria Cell

Plating technique was used to determine lowest concentration that prevent or inhibit growth of bacteria. This technique of TiO_2 nanoparticle was used against most common organisms that's cause wound infection including: MRSA, *E. coli* and *Pseudomonas aeruginosa*. Different concentrations of TiO_2 were used 100 µg/ml, 200 µg/ml, 400 µg/ml, 600 µg/ml and 800 µg/ml.

Inhibition of bacteria was different between the samples under investigation due to different physical properties and Ti/O ratios.

3.6. Antibacterial Activity of TiO_2 Nanoparticles

In this work, we used TiO_2 nanoparticles which were synthesized with novel method, and produced four samples with different O/Ti ratio. Each concentration was assayed individually in order to assess inhibitory activity against MRSA, *E. coli* and *Pseudomonas aeruginosa* and dose response manner was created.

3.6.1. Sample Ti1 of TiO_2 Nanoparticles

Antibacterial activity of TiO_2 nanoparticles were investigated against wound pathogens MRSA, *E. coli* and *Pseudomonas aeruginosa*. Experiments were performed with different concentrations at various times to determine which one of strain is effective at ambient conditions. Fig. 5 displays gradual increase of inhibition of MRSA up to 120 minutes for 100 µg/ml and 200 µg/ml concentration then inhibition was sharply increased at time 180 minutes. After that, slight increase was noticed at time 1440 minutes. However, inhibition with concentrations 400 µg/ml, 600 µg/ml and 800 µg/ml were increased gradually until 1440 minutes. Inhibitions of *Pseudomonas aeruginosa* with Ti1 sample revealed favorable effect against the growth of bacteria. At concentrations 100 µg/ml, 200 µg/ml and 400 µg/ml inhibition were increased sharply up to 120 minutes and then gradually increased up to 1440 minutes. Whereas at time 60 minutes, concentrations 600 µg/ml and 800 µg/ml exhibited highest inhibition of bacteria, then it was slightly increased up to 1440 minutes. *E. coli* exhibit also gradual inhibition until it reaches to 180 minutes then inhibition was increased sharply after 180 minutes for concentration 100 µg/ml until time 1440 minutes. Regarding the other concentrations 200 µg/ml, 400 µg/ml, 600 µg/ml and 800 µg/ml, good inhibition was observed at time 60 minutes then slightly decrease in inhibition was observed until time 180 minutes. After that, the inhibition was increased until time 1440 minutes Figure 5.

3.6.2. Sample Ti2 of TiO_2 Nanoparticles

Sample Ti2 of TiO_2 nanoparticles showed different effects with pathogenic strains that cause wound infection as shown in Figure 6. With this sample Ti2, MRSA exhibited few inhibitions at time 0 minutes, then the effect of Ti2 of TiO_2 nanoparticles was slightly decreased until time 120 minutes for concentrations 100 µg/ml, 200 µg/ml, 400 µg/ml, 600 µg/ml and 800 µg/ml. Then the inhibitory effect was increased again gradually until time 1440minutes. Regarding the inhibition of *Pseudomonas aeruginosa* by Ti2 sample concentrations 100 µg/ml, 200 µg/ml, 400 µg/ml, 600 µg/ml showed maximum inhibition until time 180 minutes. Then inhibitory effect was slightly decreased at time 1440 minutes. However, concentration 800 µg/ml showed highest inhibition at time 120minutes, then the inhibitory effect of TiO_2 shows minor increase until time 1440 minutes. *E. coli* displays different effect with each concentration, as with concentration 100µg/ml sharp inhibition of bacterial growth was observed until time 120 minutes. After that inhibitory effect was slightly decreased at time 180 minutes, then inhibition was increased again at time 1440 minute for concentration 100 µg/ml. No any effect was noticed for concentration 200µg/ml at time 0 minutes, however, after 60 minutes inhibitory effect was sharply increased until 120 minutes followed by slight increase until 1440. Other concentrations 400 µg/ml, 600 µg/ml and 800 µg/ml showed best inhibitory effect until time 60 minutes, then the inhibition was increased slightly until time 1440 minutes which has been showed Figure 6.

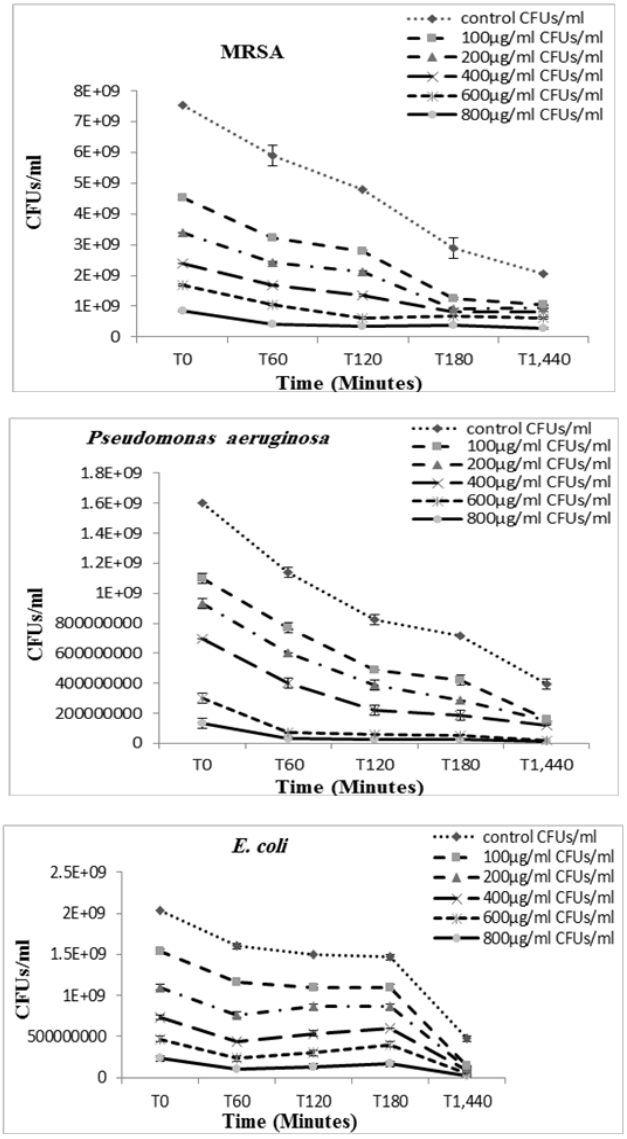

Figure 5. Effect of TiO_2 nanoparticles Ti1 with different concentration versus time on *E. coli* and *Pseudomonas aeruginosa*

3.6.3. Sample Ti3 of TiO_2 nanoparticles

Regarding the sample Ti3 of TiO_2 nanoparticles, sharp inhibitory effect was observed on MRSA until time 60 minutes with all concentrations 100 µg/ml, 200 µg/ml, 400 µg/ml, 600 µg/ml, and 800 µg/ml. Then inhibition was gradually increased until time 1440 minutes showed in Figure 7. With *Pseudomonas aeruginosa* maximum inhibitory effect was observed for all different concentrations 100 µg/ml, 200 µg/ml, 400 µg/ml, 600

μg/ml and 800 μg/ml until time 120 minutes. After that, with concentrations 100 μg/ml and 800 μg/ml showed gradual increased in inhibitory effect until time 180 minutes followed by slight decrease at time 1440 minute. Regarding the concentrations 200 μg/ml, 400 μg/ml and 600 μg/ml showed little decreased in inhibitory effect until time 1440 minutes. In *E. coli*, inhibitory effect was gradually increased until time 1440 minutes with concentrations 100 μg/ml, 200 μg/ml. Whereas with concentration 400 μg/ml inhibitory effect was gradually increased until time 60 minute, after that it showed minor decreased in inhibition until time120 minutes. A sharp increase was observed until time 180 minutes and then slight increase in inhibition was noticed at time 1440 minutes. Regarding the concentration 600 μg/ml inhibition was slightly increased until time 60 minutes. After that, inhibitory effect was slightly decreased at time 120 minutes. After 120 minutes, inhibitory effect was gradually increased until time 1440 minutes. However, with concentration 800 μg/ml inhibitory effect was increased very slightly until time 180 minutes then inhibitory effect remained the same without any obvious effect until time 1440 minutes.

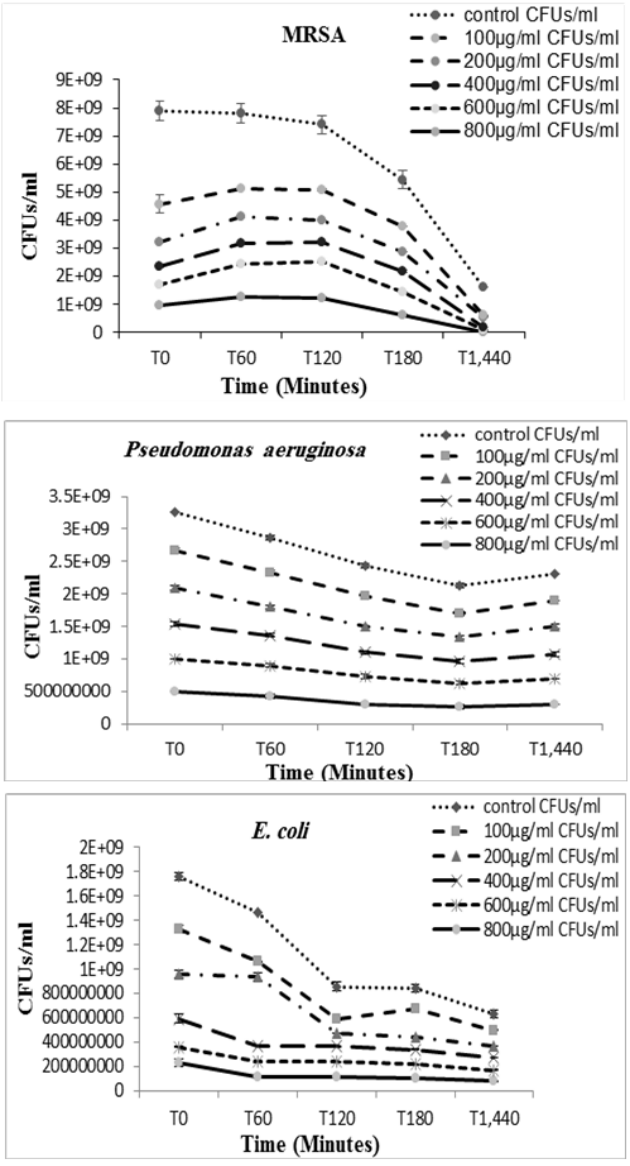

Figure 6. Effect TiO_2 quantum dot Ti2 with different concentration versus time on MRSA, *E. coli* and *Pseudomonas aeruginosa*

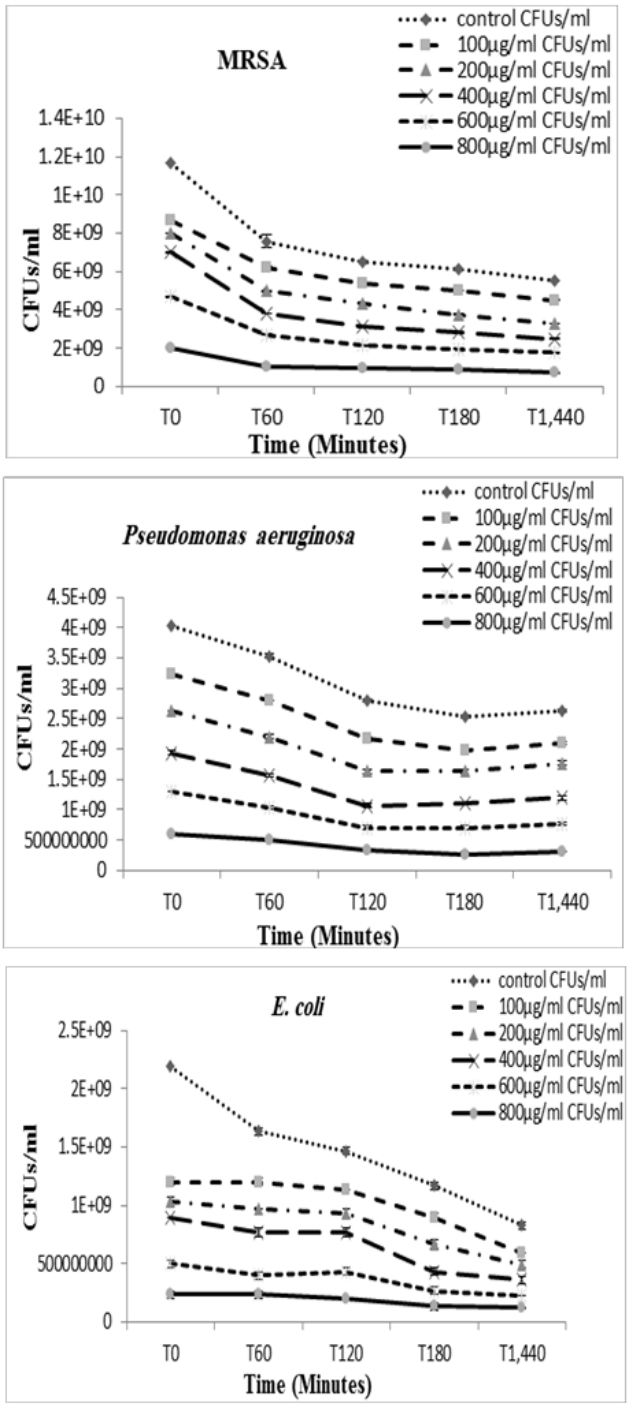

Figure 7. Effect of TiO_2 nanoparticles of Ti3 sample with different concentration versus time on MRSA, *E. coli* and *Pseudomonas aeruginosa*

3.6.4. Sample Ti4 of TiO_2 Nanoparticles

MRSA in sample Ti4 of TiO_2 nanoparticles exhibited gradual inhibitory effect until time 60 minutes with concentrations 100 μg/ml, 200 μg/ml and 400 μg/ml then inhibitory effect of TiO2 nanoparticles was slightly deceased at time 120 minutes. After that, inhibition was gradually increased until time 1440 minutes showed Figure 8.

Gradual inhibitory effect was observed with cconcentration 600 μg/ml until time 1440 minutes. Whereas with concentration 800 μg/ml inhibition was slightly increased until time 120 minutes, then sharply increased at time 180 minutes and finally slight increase was noticed at time 1440 minutes. With *Pseudomonas*

aeruginosa maximum inhibitory effect was observed with all different concentrations 100 µg/ml, 200 µg/ml 400 µg/ml, 600 µg/ml and 800 µg/ml at time 60 minutes. Then the inhibitory effect was increased slightly until time 180 minute. After that, concentrations 100 µg/ml, 200 µg/ml, 600 µg/ml and 800 µg/ml showed little decreased in inhibition at time 1440 minutes, while 400 µg/ml remained without obvious effect Fig. 9. In *E. coli* highest inhibitory effect was observed until time 60 minutes with concentrations 100 µg/ml, 200 µg/ml, 400 µg/ml, 600 µg/ml and 800 µg/ml. The concentrations 100 µg/ml, 200 µg/ml, 400 µg/ml and 600 µg/ml showed gradual increase in inhibition until time 1440 minutes, whereas with concentration 800 µg/ml inhibitory effect showed minor increased until time 1440 minutes showed Figure 8.

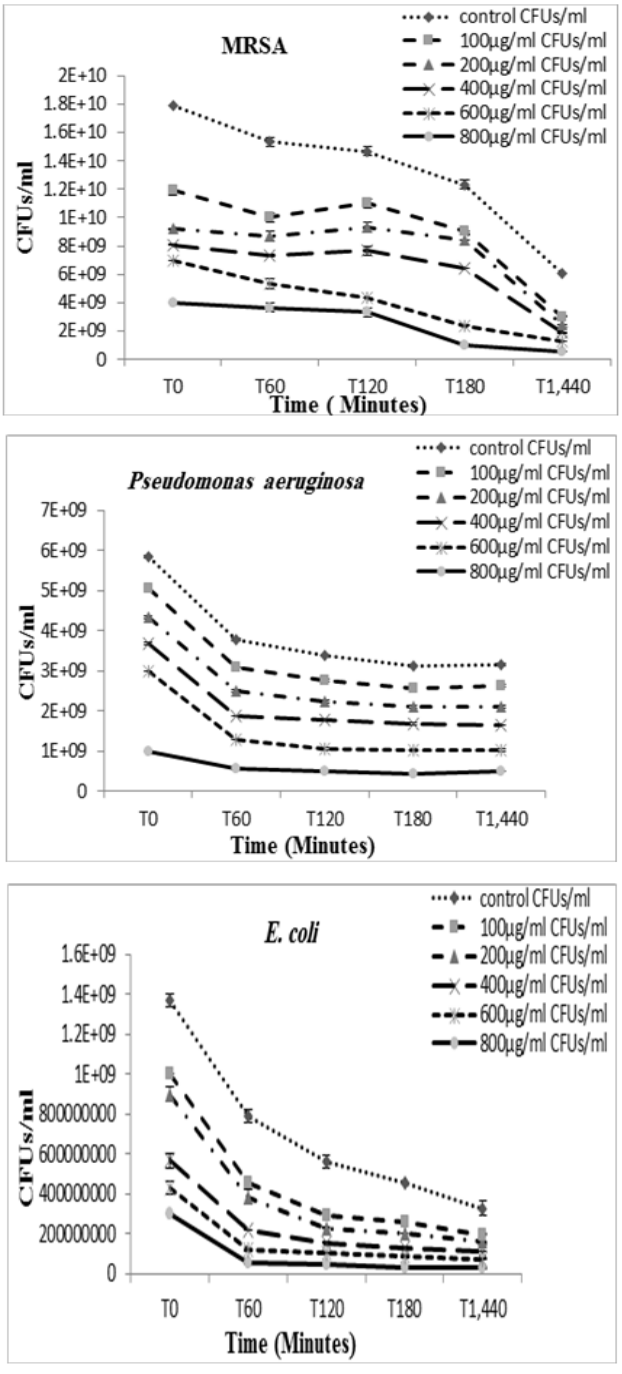

Figure 8. Effect TiO_2 nanoparticles Ti4 with different concentration versus time on MRSA, *Pseudomonas aeruginosa and E. coli*

3.7. Dose Response Curve

Antibacterial activity of TiO_2 NPs was evaluated against MRSA, *E. coli* and *Pseudomonas aeruginosa* by dose response curve analysis. Optical density was measured and plotted as a function of time for 1440 minutes at regular intervals with various concentrations of TiO_2 NPs 100 µg /ml, 200 µg /ml, 400 µg /ml, 600 µg /ml and 800 µg /ml.

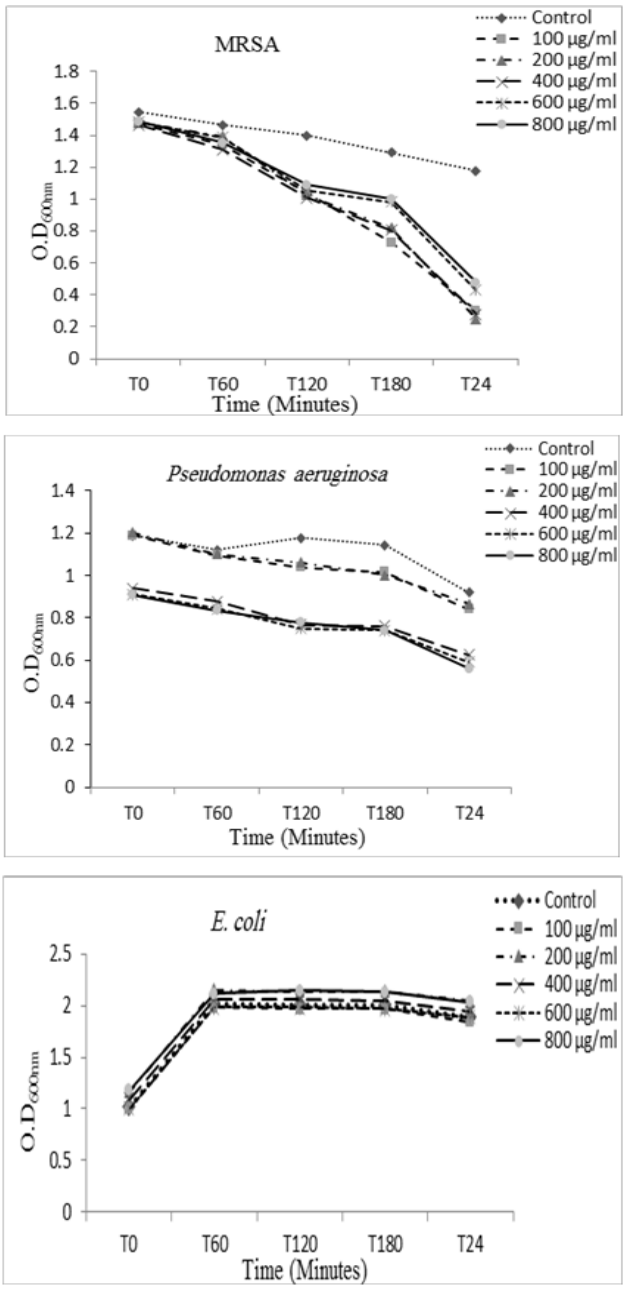

Figure 9. Dose Response curve of MRSA, *Pseudomonas aeruginosa* and *E. coli* treated with Ti1 of TiO_2-NPs at different concentrations(µg/ml) versus time

3.7.1. Dose Response Curve of Sample Ti1

Dose Response Curve of bacteria that was treated with TiO_2 nanoparticles indicated that, inhibitory effect of TiO_2 nanoparticles was different between species and from sample to sample. Dose response curve of MRSA, *E. coli* and *Pseudomonas aeruginosa* treated with TiO_2 sample Ti1 are shown in Figure 9. Dose response curve of MRSA

observed that, optical density of bacterial growth was decreased with increasing the concentrations of TiO_2 NPs. In the absence of TiO_2 NPs, optical density was increased, indicating that bacterial growth was increased, but as the TiO_2 NPs concentration was increased, optical density decreased, showing the reduction of bacterial growth rate. With this sample, lowest concentration 100 µg /ml, 200 µg /ml and 400 µg /ml were exhibited high reduction in bacterial growth rate. Dose response curve of *Pseudomonas aeruginosa* showed that, optical density of bacterial growth was decreased with increase in the concentration of TiO_2. Resulting the increased reduction of bacterial growth rate. Dose response curve of *E. coli* showed very little effect of different concentrations of sample Ti1 of TiO_2 nanoparticles on the growth of bacterial cell rate and consequently, optical density of bacterial growth shows very little decreased with increased concentration.

3.7.2. Dose Response Curve of Sample Ti2

Regarding the effect of sample Ti2 of TiO_2 nanoparticles on MRSA, Dose response curve showed that the optical density of bacterial growth was decreased with increasing the concentration of TiO_2, resulting the increased reduction of bacterial growth rate. The sample concentrations 400 µg/ml and 600 µg/ml exhibited highest reduction of bacterial growth rate shown in Figure 10. Dose response curve of *Pseudomonas aeruginosa* showed that, optical density of bacterial growth was decreased with increasing the concentration of TiO_2, resulting in the increased reduction of bacterial growth rate. In case of *E. coli*, dose response curve showed that the optical density of bacterial growth was decreased with increasing the concentration of TiO_2, resulting in the increased reduction of bacterial growth rate.

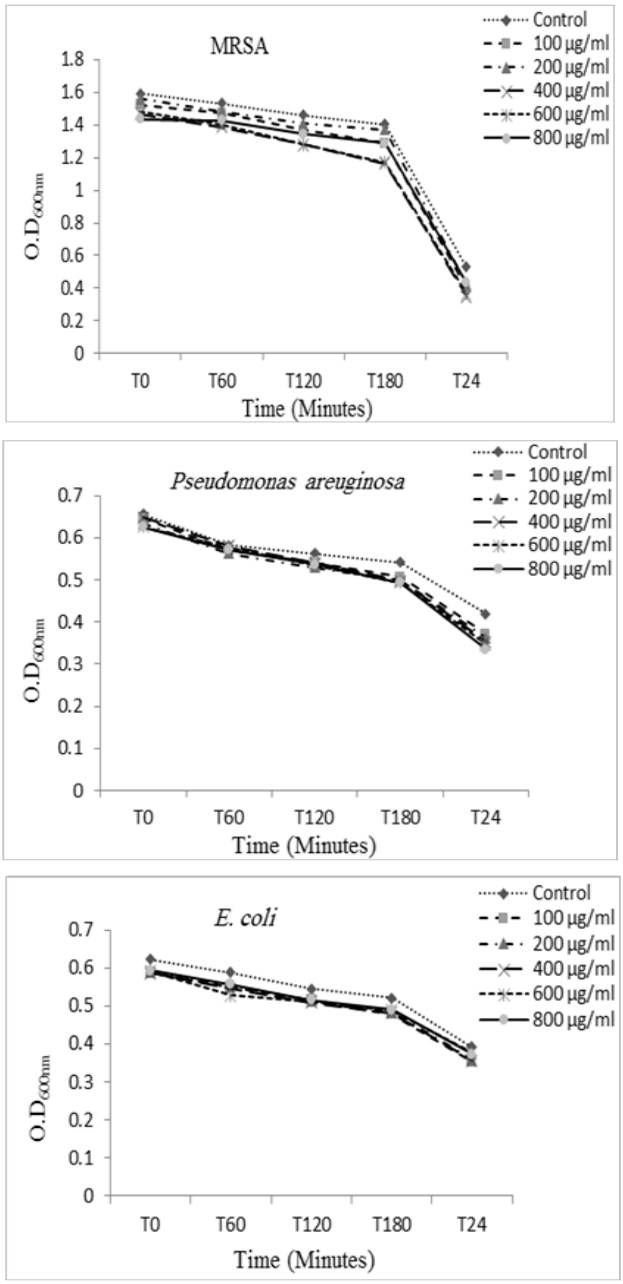

Figure 10. Dose Response curve of MRSA, *Pseudomonas aeruginosa* and *E. coli* treated with Ti2 of TiO_2-NPs at different concentrations (µg/ml) versus time

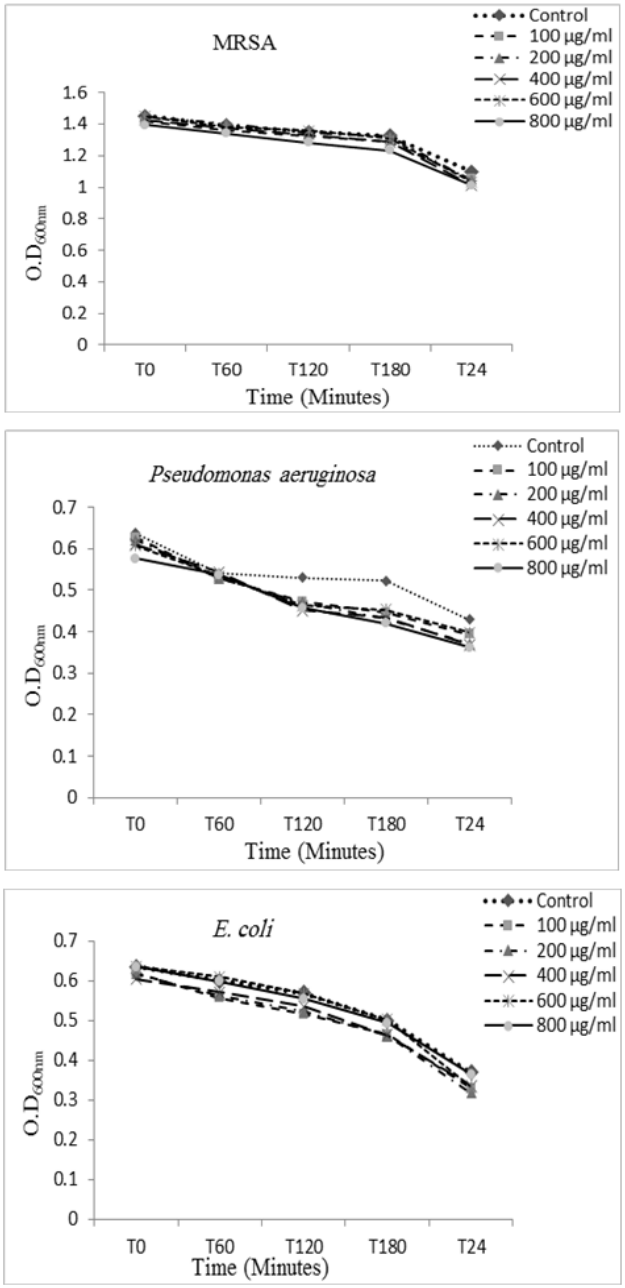

Figure 11. Dose Response curve of MRSA, *Pseudomonas aeruginosa* and *E. coli* treated with Ti3 of TiO_2-NPs at different concentrations (µg/ml) versus time

3.7.3. Dose Response Curve of Sample Ti3

Dose Response Curve of MRSA observed that, optical density of bacterial growth was decreased with increasing the concentration of TiO_2 resulting in the increased reduction of bacterial growth rate. Also, Dose Response Curve of *Pseudomonas aeruginosa* showed the optical density of bacterial growth was decreased with increasing the TiO_2 concentration, resulting in the increased reduction of bacterial growth rate shown Figure 11. Dose Response Curve of *E. coli* showed that the optical density of bacterial growth was decreased with increasing the concentration of TiO_2, resulting in the increased reduction of bacterial growth rate. Specially, with concentrations 100 µg/ml, 200 µg/ml and 400 µg/ml, optical density was considerably decreased resulting in the increased reduction growth rate of bacterial cell.

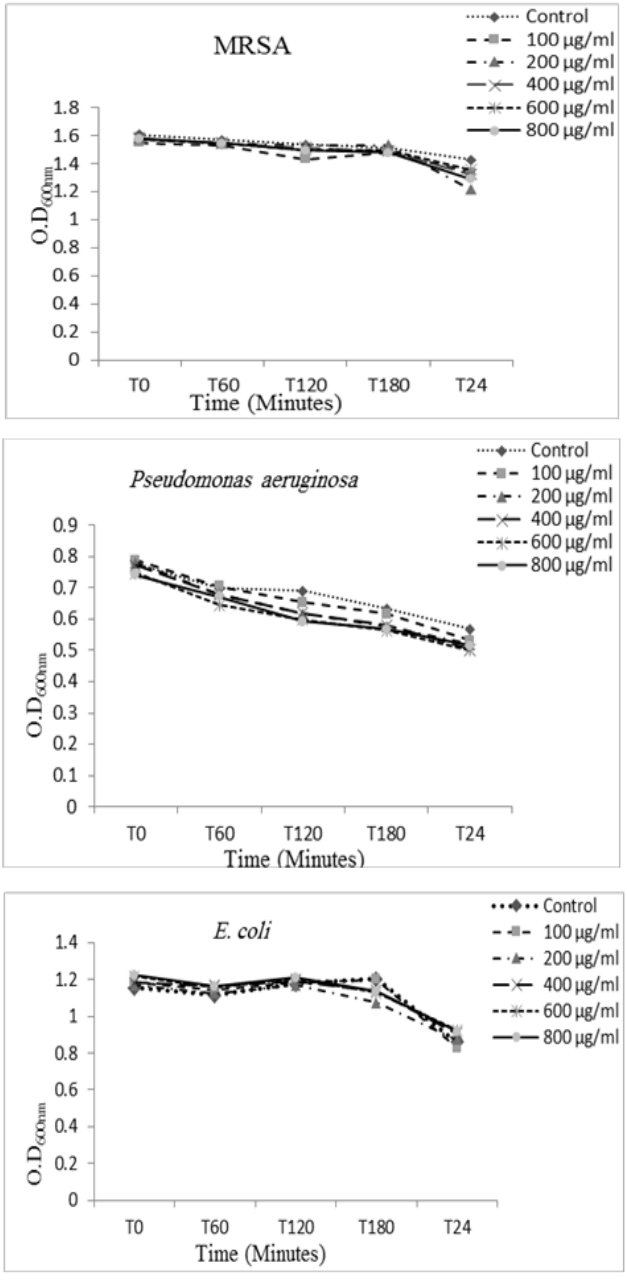

Figure 12. Dose Response curve of MRSA, *Pseudomonas aeruginosa* and *E. coli* treated with Ti4 of TiO_2-NPs at different concentrations (µg/ml) versus time

3.7.4. Dose Response Curve of Sample Ti4

In sample Ti4, dose response curve of MRSA showed little effect of different concentrations of sample Ti4 of TiO_2 on growth rate of bacterial cell, resulting in the minor decreasing effect of optical density of bacterial growth with increased concentration. However, dose response curve of *Pseudomonas aeruginosa* showed, optical density of bacterial growth was decreased with increasing the concentration of TiO_2, resulting in the increased reduction of bacterial growth rate. Dose Response Curve of *E. coli* showed very negligible effect of different concentrations on the growth rate of bacterial cell. While, with concentration 200 µg/ml, optical density was considerably decreased compared to the other concentrations, resulting in the increased reduction of growth rate of bacterial cell shown in Figure 12.

4. Discussion

In this work, effect of anatase structure of TiO_2 nanocrystallites with varied sizes on the inhibition of MRSA, *E. coli* and *Pseudomonas aeruginosa* at ambient condition were investigated. These kinds of bacteria are the most resistant to most of the antibiotics and can be considered as most effective agents of nosocomial infections. Consequently, introducing the new antibacterial agents can control the rate of morbidity and mortality that caused by the infectious diseases. It's known that bulk TiO_2 is one of the effective materials in killing microbial cells. Also, effect of bulk TiO_2 in killing of cancer cells has also been reported. On the other hand, TiO_2 nanostructure showed a strong inhibiting effect towards a various type of bacterial strains. The nanostructures have distinct properties like increase surface per volume ratio and carrier life time which are effective on inhibition of bacterial activity.

XRD and UV-vis absorption proved a change in particles sizes and optical band gap. The effect of nanocrystallite on inhibition of pathogenic strains that lead to wound infection can be concluded as follow. The nanoparticles with larger sizes are more influencing on inhibition of MRSA bacteria more than the smaller one. However, the smaller nanocrystallites sizes are more effective for inhibition of *Pseudomonas aeruginosa* and *E. coli*. As the size of nanocrystallite increase the surface per volume ratio decrease and a gradual change on optical properties and physical properties, consequently the effect of inhibition should change with changing nanoparticles sizes. Also, the increase of activity of inhibition for smaller particles for *Pseudomonas aeruginosa* and *E. coli* relative to MRSA inhibition may reflect that the binding of nanoparticless to *Pseudomonas aeruginosa* and *E. coli* are different in comparison with the binding of nanoparticless with MRSA. The binding of nanocrystallites with bacterial cells effects on the movement, growth and cell death due to hemostatic imbalance and cellular metabolic disturbance. Moreover, the attachment of nanocrystallite with the cell influence on the production of intracellular reactive oxygen species (ROS). Previous study showed that the coordination and surface properties allow anatase after dispersion induce the generation of ROS [34].

Another important result from the effect of nanoparticless on various kinds of bacteria is the ability of penetration in the cells, we expect that the penetration of smaller nanoparticless into *Pseudomonas aeruginosa* and *E. coli* are more effective in comparison with the penetration of smaller nanoparticless into MRSA. The penetration of nanocrysttalite can deactivate biomolecules such as proteins.

According to elemental analysis the nanocrystallites with low O/Ti weight percentage are more effective for inhibition of *E. coli* and *Pseudomonas aeruginosa*, which indicates that the increase of Ti ions at the surface of nanocrystallites is one of the factor of antibacterial activity of TiO_2 against *Pseudomonas aeruginosa* and *E. coli* strains. However, the nanocrystallites with high O/Ti weight percentage are more effective against inhibition of growth of MRSA, which indicate that the presence of oxygen species on the surface of nanocrystalites is one of the factor that important for antibacterial activity of TiO_2 against MRSA strain.

The effect of TiO_2 concentration on the inhibtion of growth of the three strains MRSA, *E. coli* and *Pseudomonas aeruginosa* were investigated. The smallest nanocrystallite size showed a pronounced inhibitory effect and high reduction of growth rate of bacteria with increasing the concentrations of TiO_2 nanocrystallites for the three strains of bacteria.

According to above results the different concentrations of TiO_2 smallest crystallits could inhibit the growth of antibiotic resistant three strains of MRSA, *Pseudomonas aeruginosa* and *E. coli*. Consequently, the prepared nanostructures could be considered as excellent alternative treatment for Drug-resistant bacterial infections.

Acknowledgements

This project was funded by King Abdulaziz City for Science and Technology (KACST) at Saudi Arabia, under postgraduate students grants. The authors, therefore, acknowledge with thanks KACST for technical and financial support.

References

[1] A. L. Linsebigler, G. Lu, and J. T. Yates, "Photocatalysis on TiO_2 Surfaces: Principles, Mechanisms, and Selected Results," *Chem Rev*, vol. 95, pp. 735-758, May1995.

[2] C. Aprile, E. Gobechiya, J. A. Martens, and P. P. Pescarmona, "New mesoporous composites of gallia nanoparticles: high-throughput synthesis and catalytic application," *Chemical Communications*, vol. 46, pp. 7712-7714, Sep 2010.

[3] Manoj A. Lazar and S. V. a. S. S. Nair, "Photocatalytic Water Treatment by Titanium Dioxide," *MDPI"*, vol. 2 (4): 572-601. 2012.

[4] S. M. Dizaj, F. Lotfipour, M. Barzegar-Jalali, M. H. Zarrintan, and K. Adibkia, "Antimicrobial activity of the metals and metal oxide nanoparticles," *Mater Sci Eng C Mater Biol Appl*, vol. 44, pp. 278-84, Nov 2014.

[5] P. Singh, M. Abdullah, and S. Ikram, "Role of Nanomaterials and their Applications as Photo-catalyst and Senors: A Review," *Nano Research & Applications, vol. 2:10,* Dec 2015.

[6] D. F. Ollis and H. Al-Ekabi, Photocatalytic purification and treatment of water and air*:* proceedings of the *1st International Conference on TiO_2 Photocatalytic Purification and Treatment of Water and Air*, Elsevier Science Ltd, 8-13.

[7] S. Wageh, "Light Emitting Devices Based on CdSe Nanoparticles Capped With Mercaptoacetic Acid," *IEEE Journal of Quantum Electronics*, vol. 50, pp. 1-8, Sep 2014.

[8] X. Wu, H. Liu, J. Liu, K. N. Haley, J. A. Treadway, J. P. Larson, N. Ge, F. Peale, and M. P. Bruchez, "Immunofluorescent labeling of cancer marker Her2 and other cellular targets with semiconductor quantum dots," *Nat Biotechnol*, vol. 21, pp. 41-6, Jan 2003.

[9] J. D. Fortner, D. Y. Lyon, C. M. Sayes, A. M. Boyd, J. C. Falkner, E. M. Hotze, L. B. Alemany, Y. J. Tao, W. Guo, K. D. Ausman, V. L. Colvin, and J. B. Hughes, "C60 in Water: Nanocrystal Formation and Microbial Response," *Environmental Science & Technology*, vol. 39, pp. 4307-4316, Apr 2005.

[10] A. Chwalibog, E. Sawosz, A. Hotowy, J. Szeliga, S. Mitura, K. Mitura, M. Grodzik, P. Orlowski, and A. Sokolowska, "Visualization of interaction between inorganic nanoparticles and bacteria or fungi," *Int J Nanomedicine*, vol. 5, pp. 1085-1094, Dec 2010.

[11] E. C. Wang and A. Z. Wang, "Nanoparticles and their applications in cell and molecular biology," *Integr Biol (Camb)*, vol. 6, pp. 9-26, Jan 2014.

[12] M. C. Daniel and D. Astruc, "Gold nanoparticles: assembly, supramolecular chemistry, quantum-size-related properties, and applications toward biology, catalysis, and nanotechnology," *Chem Rev*, vol. 104, pp. 293-346, Jan 2004.

[13] A. N. Banerjee, "The design, fabrication, and photocatalytic utility of nanostructured semiconductors: focus on TiO_2" *Nanotechnology, science and applications*, vol. 4, pp. 35-65, Feb 2011.

[14] N. Beyth, Y. Houri-Haddad, A. Domb, W. Khan, and R. Hazan, "Alternative antimicrobial approach: nano-antimicrobial materials," *Evidence-Based Complementary and Alternative Medicine*, vol. 2015, Mar 2015.

[15] N. Bahadur, K. Jain, R. Pasricha, and S. Chand, "Selective gas sensing response from different loading of Ag in sol–gel mesoporous titania powders," *Sensors and Actuators B: Chemical*, vol. 159, pp. 112-120, Jun 2011.

[16] S. Mahshid, M. S. Ghamsari, M. Askari, N. Afshar, and S. Lahuti, "Synthesis of TiO_2 nanoparticles by hydrolysis and peptization of titanium isopropoxide solution," *Semiconductor Physics, Quantum Electronics & Optoelectronics*, vol. 9, pp. 65-68, Jul 2006.

[17] P. Anandgaonker, G. Kulkarni, S. Gaikwad, and A. Rajbhoj, "Synthesis of TiO_2 nanoparticles by electrochemical method and their antibacterial application," *Arabian Journal of Chemistry*, Jan 2015.

[18] X. Shen, J. Zhang, and B. Tian, "Microemulsion-mediated solvothermal synthesis and photocatalytic properties of crystalline titania with controllable phases of anatase and rutile," *Journal of hazardous materials*, vol. 192, pp. 651-657, Aug 2011.

[19] S. Kasap, H. Tel, and S. Piskin, "Preparation of TiO_2 nanoparticles by sonochemical method, isotherm, thermodynamic and kinetic studies on the sorption of strontium," *Journal of Radioanalytical and Nuclear Chemistry*, vol. 289, pp. 489-495, Aug 2011.

[20] S. Samal, D.-W. Kim, K.-S. Kim, and D.-W. Park, "Direct synthesis of TiO_2 nanoparticles by using the solid-state precursor TiH2 powder in a thermal plasma reactor," *Chemical Engineering Research and Design*, vol. 90, pp. 1074-1081, Aug 2012.

[21] K. Ding, Z. Miao, Z. Liu, Z. Zhang, B. Han, G. An, S. Miao, and Y. Xie, "Facile synthesis of high quality TiO_2 nanocrystals in ionic liquid via a microwave-assisted process," *Journal of the American Chemical Society*, vol. 129, pp. 6362-6363, May 2007.

[22] M. Zarei, A. Jamnejad, and E. Khajehali, "Antibacterial effect of silver nanoparticles against four foodborne pathogens," *Jundishapur Journal of Microbiology*, vol. 7, Jan 2014.

[23] M. A. Vetten, C. S. Yah, T. Singh, and M. Gulumian, "Challenges facing sterilization and depyrogenation of nanoparticles: effects on structural stability and biomedical applications," *Nanomedicine: Nanotechnology, Biology and Medicine*, vol. 10, pp. 1391-1399, Mar 2014.

[24] B. Fritz, D. K. Walker, D. Goveia, A. E. Parker, and D. M. Goeres, "Evaluation of Petrifilm™ Aerobic Count Plates as an Equivalent Alternative to Drop Plating on R2A Agar Plates in a Biofilm Disinfectant Efficacy Test," *Current microbiology*, vol. 70, pp. 450-456, Mar 2015.

[25] M. Ng, S. B. Epstein, M. T. Callahan, B. O. Piotrowski, G. L. Simon, A. D. Roberts, J. F. Keiser, and J. B. Kaplan, "Induction of MRSA biofilm by low-dose β-lactam antibiotics: specificity, prevalence and dose-response effects," *Dose-Response*, vol. 12, pp. dose-response. 13-021, Jan 2014.

[26] M. D. Rolfe, C. J. Rice, S. Lucchini, C. Pin, A. Thompson, A. D. Cameron, M. Alston, M. F. Stringer, R. P. Betts, and J. Baranyi, "Lag phase is a distinct growth phase that prepares bacteria for exponential growth and involves transient metal accumulation," *Journal of bacteriology*, vol. 194, pp. 686-701, Feb 2012.

[27] J. M. N. Llorens, A. Tormo, and E. Martínez-García, "Stationary phase in gram-negative bacteria," *FEMS microbiology reviews*, vol. 34, pp. 476-495, Jun 2010.

[28] N. V. Pletneva, V. Z. Pletnev, K. S. Sarkisyan, D. A. Gorbachev, E. S. Egorov, A. S. Mishin, K. A. Lukyanov, Z. Dauter, and S. Pletnev, "Crystal structure of phototoxic orange fluorescent proteins with a tryptophan-based chromophore," *PloS one*, vol. 10, p. e0145740, Dec 2015.

[29] L. Helmus, R. K. Hanson, D. Thornton, K. M. Babchishin, and A. J. Harris, "Absolute recidivism rates predicted by Static-99R and Static-2002R sex offender risk assessment tools vary across samples a meta-analysis," *Criminal justice and behavior*, vol. 39, pp. 1148-1171, May 2012.

[30] S.-H. Kim, H.-S. Lee, D.-S. Ryu, S.-J. Choi, and D.-S. Lee, "Antibacterial activity of silver-nanoparticles against Staphylococcus aureus and Escherichia coli," *Korean J. Microbiol. Biotechnol*, vol. 39, pp. 77-85, Fep 2011.

[31] S. Valencia, J. M. Marín, and G. Restrepo, "Study of the bandgap of synthesized titanium dioxide nanoparticules using the sol-gel method and a hydrothermal treatment," *Open Materials Science Journal*, vol. 4, pp. 9-14, Apr 2010.

[32] M. A. Islam, M. J. Haither, I. Khan, and M. Islam, "Optical and Structura l Characterization of TiO_2 Nanoparticles," *IOSR J. Electr. Electron. Eng.*, vol. 3 (2), PP 18-24, Nov.-Dec 2012.

[33] T. Matsumoto, J.-i. Suzuki, M. Ohnuma, Y. Kanemitsu, and Y. Masumoto, "Evidence of quantum size effect in nanocrystalline silicon by optical absorption," *Physical review B*, vol. 63, p. 195322, May 2001.

[34] L. Clément, C. Hurel, and N. Marmier, "Toxicity of TiO_2 nanoparticles to cladocerans, algae, rotifers and plants–effects of size and crystalline structure," *Chemosphere*, vol. 90, pp. 1083-1090, Jan 2013.